Static stability of pendent drops pinned to arbitrary closed curves

X. Lin, L. E. Johns, and R. Narayanan*
Department of Chemical Engineering, University of Florida, Gainesville, Florida 32611, USA
(Received 25 May 2016; published 27 November 2017)

We compare the stability of a static pendent drop under two types of control, volume control and pressure control. The drops are taken to be pinned to curves of arbitrary shape. The two types of control introduce integrals into the eigenvalue problems that determine the points of instability. We show that these integrals are solely responsible for the possible occurrence of bifurcation points, depending only on the Bond number. We then show that the points of instability for either type of control can be related to one another and predicted precisely from the eigenvalues of, yet, a third problem, one that is devoid of any integrals. If the curves of attachment are symmetric, we can derive a result that predicts the instability point and associated pattern, all without solving any eigenvalue problem.

DOI: 10.1103/PhysRevFluids.2.113605

I. INTRODUCTION

A pendent drop is an equilibrium configuration that reaches a point of instability as its volume or its pressure is increased [1–4]. A pendent drop's point of instability depends on the opposition of gravity and curvature. We are going to deal with the stability of static drops pinned at their edges. We do not ask what happens beyond the point of instability, but we can guess the patterns at breakup, a pattern that can be observed.

The equilibrium shape or base shape of a drop depends on its volume or its pressure, given the density difference, the surface tension, and the diameter of its closed curve of attachment. The shape then determines the point of instability, and hence variational methods seeking the least potential energy have been used to first determine the shape and then to learn if the shape is stable, i.e., to learn that drops pinned to circles break in a symmetrical pattern at their greatest volume.

Now, it has been thought since Maxwell's time that drops at small volumes ought to break in unsymmetrical patterns. Because drops start their lives as plane surfaces pinned at their edges, supporting a heavy fluid lying above a light fluid, where gravity is destabilizing and surface tension is stabilizing, their stability is determined by solving the Rayleigh-Taylor problem, and this problem has been solved by Maxwell [5], for plane surfaces pinned to circles or to rectangles. In the case of circles, Maxwell finds that the shape of the surface at the point of instability is not symmetric about the axis. Hence this is the expectation for drops of small volume even though a symmetric pattern is expected at large volumes.

The volume or the pressure at the point of instability depends on the Bond number, a dimensionless group made up of the density difference, the surface tension, and the diameter of the cross section, and there is a Bond number at which a planar surface becomes unstable. A drop experiment is run by setting the Bond number less than its critical value for a plane surface and increasing the volume or the pressure until a point of instability is reached.

The shape of symmetric drops pinned at their edges and their stability have been determined by the calculations being carried out by variational methods [6–8]. At each volume, the shape corresponds to the least potential energy, and stability is predicted if the potential energy increases on imposing a symmetric perturbation. Upon increasing the volume the drop reaches a volume where the potential energy no longer increases on introducing a symmetric perturbation. A critical point has been reached. The volume can no longer be increased, and the drop has reached its greatest possible volume.

*Corresponding author: ranga@ufl.edu

It may be that upon imposing an unsymmetrical perturbation, an instability will be found at a volume less than the greatest volume. If this is the case, the critical point at the lower volume will be a bifurcation point, due to the fact that a drop shape can be computed even if the volume is increased through this point. Bifurcation points have found for drops pinned to circles, and it is known that at bifurcation points contact at the edge is horizontal [9].

At each point along the path of increasing volume or pressure, at a given Bond number, we can discover whether the drop is stable to small perturbations by first finding its shape and then solving an eigenvalue problem based on the shape. A critical point is reached when one of the eigenvalues becomes equal to the Bond number. The pattern seen at breakup then depends on which eigenvalue reaches the Bond number first.

Integrals appear in these eigenvalue problems due to constraints on the allowed perturbations. These integrals account for the difference between volume-controlled and pressure-controlled experiments and for differences seen in either experiment which depend on the Bond number.

There is a limiting, but not uncommon, pressure-controlled experiment, an experiment of physical interest, in which no integrals appear in the corresponding eigenvalue problem. We refer to this as a diffusion eigenvalue problem and find that the eigenvalues for all other drop stability problems can be derived from the diffusion eigenvalues and hence can be connected to one another.

The shape of the cross section is a variable of interest, and we start with a more or less arbitrary shape. Then we move on to more symmetric shapes. Upon increasing symmetry we come to cross sections where certain diffusion eigenvalues become critical points of other drop problems, leading, if there is enough symmetry, to predictions of bifurcation points from the base shape itself.

Thus, say, for a drop pinned to a circle, as the volume increases, from the drop shapes and a plot of the drop volume versus the pressure, and nothing more, we can find the maximum volume, i.e., the turning point, and we can say whether of not there is a bifurcation point appearing before the turning point, and if there is, at what volume it appears.

Our view is that the problem of finding critical points is hydrostatic. There is no dynamics. This is explained in Appendices A and B where we prove that if the real part of the growth constant vanishes, so too the imaginary part, assuming the viscosity is not zero. Hence if we were running an experiment, we would creep up slowly on the critical point by increasing the volume or the pressure.

Our plan is to introduce models for two thought experiments, one for drops under volume control, called experiment I, and the other for drops under pressure control, called experiment II. We call these experiments thought experiments because they are to be used to guide real experiments. After presenting what we find for drops pinned to arbitrary curves, we write a one-dimensional model, i.e., a model where the drop shape depends on only one independent variable, where the drop is pinned to two points and where there is only one curvature. This model predicts all the qualitative results that are known about drops pinned to circles, including the fact that there is a discontinuous change in the pattern of the instability at critical as the Bond number decreases, an abrupt change not seen in the case of a drop pinned to an arbitrary closed curve, notwithstanding the fact that drops pinned to circles have two curvatures. The odd and even eigenfunctions in the one-dimensional model correspond to $m = 0$ and $m = 1$ eigenfunctions in the case of circular symmetry.

Our assumptions are (1) the drop is pinned to a closed horizontal curve and (2) the critical points can be identified by a static perturbation. The second is proved in Appendices A and B and is an application of the Rayleigh work principle [10]. The first, pinned edges, is supported by Mason [11], who, in an experiment, obtained a critical bridge length equal to the circumference of the bridge, a pinned-edge result.

II. ARBITRARY CROSS SECTIONS

A. Volume control

Figure 1 illustrates a static pendent drop, pinned along a curve $\mathcal{C}$ bounding a cross section $\mathcal{A}$ of area A. We denote the shape of the drop by $z = Z(x, y)$, and we write our equations for Z in scaled variables, introducing the Bond number, denoted B, where $B = \frac{\Delta \rho g}{\gamma} D^2$, where $\Delta \rho = \rho - \rho*$,

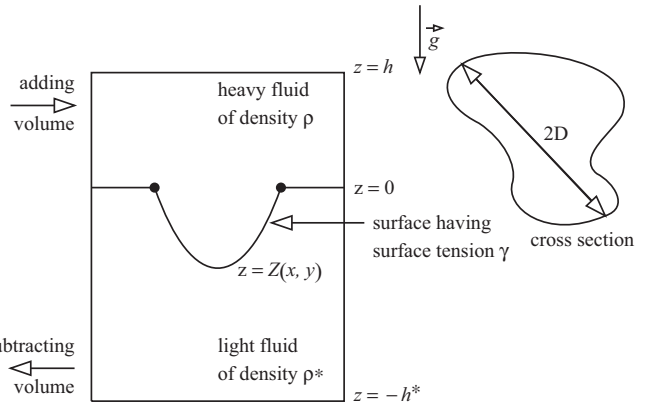

FIG. 1. A sketch of a drop pinned along a curve, $\mathcal{C}$, bounding a cross section, $\mathcal{A}$, under volume control, experiment I.

where D denotes half the diameter of $\mathcal{A}$ and where all lengths are scaled by D. The origin of our coordinate system lies in the plane of $\mathcal{A}$ with z measured upward.

The assumption that we can express the shape $z = Z(x,y)$ [or $z = Z(r,\theta)$] cannot be true if the Bond number is small. Thus if B is near zero we write $z = R(\theta,z)$ for $z^* < z < 0$ and $z = Z(r,\theta)$ for $z < z^*$ and glue the two pieces together at $z = z^*$. This is explained elsewhere [12].

Our model, derived unscaled in Appendix E, is

$$P - BZ = \nabla \cdot \frac{\nabla Z}{(1 + \nabla Z \cdot \nabla Z)^{1/2}}, \tag{1}$$

$$Z = 0 \quad \text{along} \quad \mathcal{C}, \tag{2}$$

and

$$\iint_{\mathcal{A}} Z \, dx \, dy = -V, \tag{3}$$

where P denotes the scaled value of $P_{\text{top}} + \rho g h + \rho * g h^* - P_{\text{bottom}}$ and $P_{\text{top}} = P(z = h)$, etc.

In our first experiment B and V are input variables where V denotes the volume of the drop. The outputs are $Z(x,y)$ and P. At $V = 0$ we have $Z = 0$ and $P = 0$. Now B is our primary control variable, and, setting a value of B, we increase V and we wish to know if the drop is stable to small perturbations at each V along the way.

Our aim is to write the perturbation problem at zero growth rate and identify conditions where this problem has solutions other than zero. The static perturbation problem at constant B and V is

$$P_1 - BZ_1 = \mathcal{L}Z_1 = 2H_1, \tag{4}$$

$$Z_1 = 0 \quad \text{on} \quad \mathcal{C}, \tag{5}$$

and

$$\iint_{\mathcal{A}} Z_1 \, dx \, dy = 0, \tag{6}$$

where

$$\mathcal{L} = \nabla \cdot \left\{ \frac{\overrightarrow{\overrightarrow{I}}\,(1 + \nabla Z \cdot \nabla Z) - \nabla Z \nabla Z}{(1 + \nabla Z \cdot \nabla Z)^{3/2}} \cdot \nabla \right\} \tag{7}$$

and where Z denotes the solution to Eqs. (1)–(3) at the B and V of interest.

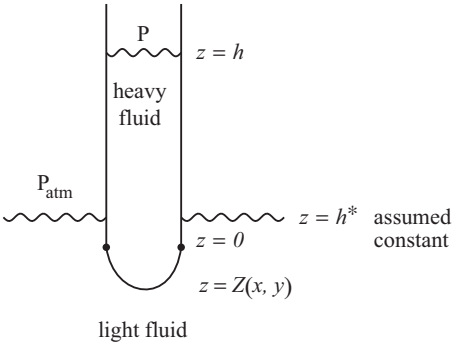

FIG. 2. A sketch of a drop under pressure control, experiment II.

The perturbation problem is homogeneous, and we seek steady solutions Z_1, not zero. In Appendix A we prove that if the real part of the growth constant corresponding to a time-dependent perturbation is zero, so too the imaginary part. In Appendix B we prove that a nonzero static perturbation causes the potential energy of the drop to decrease.

As we advance V we wish to know whether or not there is a limit, i.e., a greatest value of V. So at an input B and V, and a drop shape, Z, we wish to know if we can obtain $\dot{Z} = \frac{dZ}{dV}$. The problem to be solved, obtained by differentiating Eqs. (1)–(3), is

$$\dot{P} - B\,\dot{Z} = \mathcal{L}\,\dot{Z}, \tag{8}$$

$$\dot{Z} = 0 \quad \text{on} \quad \mathcal{C}, \tag{9}$$

and

$$\iint_{\mathcal{A}} \dot{Z}\, dx\, dy = -1. \tag{10}$$

B. Pressure control

In experiment I, V is an input. In experiment II (cf. Fig. 2) V is an output, and P is now an input. Our model in experiment II is

$$P + B^* \frac{1}{A} \iint_{\mathcal{A}} Z\, dx\, dy - BZ = \nabla \cdot \frac{\nabla Z}{(1 + \nabla Z \cdot \nabla Z)^{1/2}}, \tag{11}$$

$$Z = 0 \quad \text{along} \quad \mathcal{C}, \tag{12}$$

and

$$\iint_{\mathcal{A}} Z\, dx\, dy = -V, \tag{13}$$

where $B^* = \frac{\rho g D^2}{\gamma} > B$.

The inputs are P, B^*, and B, the outputs are $Z(x, y)$ and V. At $P = 0$ we have $Z = 0$ and $V = 0$. If we need to distinguish variables in experiment I from those in experiment II we will introduce the labels I and II. In Eq. (11) P denotes the scaled difference $P - P_0$, and the integral $\frac{1}{A}\iint_{\mathcal{A}} Z\, dx\, dy$ accounts for the difference $(h - h_0)$, where P_0 and h_0 correspond to $Z = 0$. The integral is important. It accounts for the fact that the total volume of heavy fluid remains constant.

Again B is our primary control variable and, setting a value of B, we increase P, and we wish to know if the drop is stable to small perturbations at each P along the way. The perturbation problem

at constant B and P is

$$B^* \frac{1}{A} \iint_{\mathcal{A}} Z_1 \, dx \, dy - B Z_1 = \mathcal{L} Z_1 \tag{14}$$

and

$$Z_1 = 0 \quad \text{on} \quad \mathcal{C}, \tag{15}$$

where $\iint_{\mathcal{A}} Z_1 \, dx \, dy = -V_1$, and as we advance P we wish to know if there is a bound, i.e., a greatest value of P. Therefore, we wish to know if, at an input B and P, and therefore Z, we can find $\dot{Z} = \frac{dZ}{dP}$ where the problem to be solved for $\dot{Z}$ is

$$1 + B^* \frac{1}{A} \iint_{\mathcal{A}} \dot{Z} \, dx \, dy - B \dot{Z} = \mathcal{L} \dot{Z}, \tag{16}$$

and

$$\dot{Z} = 0 \quad \text{on} \quad \mathcal{C}, \tag{17}$$

where $\iint_{\mathcal{A}} \dot{Z} \, dx \, dy = -\dot{V}$

C. Eigenvalue problems for volume and pressure control

Associated with the perturbation problem at constant B and V, viz., Eqs. (4)–(6), we have the eigenvalue problem

$$C - \lambda^2 \psi = \mathcal{L} \psi, \tag{18}$$

$$\psi = 0 \quad \text{on} \quad \mathcal{C}, \tag{19}$$

and

$$\iint_{\mathcal{A}} \psi \, dx \, dy = 0. \tag{20}$$

We denote its solutions λ^2, ψ, and C and observe that the perturbation problem at constant B and V has a solution $Z_1 \neq 0$ if and only if one of the λ^2 satisfying Eqs. (18)–(20) is equal to B.

Likewise we associate an eigenvalue problem with the perturbation problem at constant B and P, *viz.,* Eqs. (14) and (15):

$$B^* \frac{1}{A} \iint_{\mathcal{A}} \psi \, dx \, dy - \lambda^2 \psi = \mathcal{L} \psi \tag{21}$$

and

$$\psi = 0 \quad \text{on} \quad \mathcal{C}, \tag{22}$$

and we denote its solutions λ^2, ψ, and again we observe that the perturbation problem at constant B and P has a solution $Z_1 \neq 0$ if and only if one of the λ^2 satisfying Eqs. (21) and (22) equals B.

The integrals appearing in Eqs. (20) and (21) account for the way experiments I and II differ and for the way both experiments differ from the pressure-controlled experiment proposed by Wente [13]. In that experiment the fundamental eigenfunction is singly signed and the first neutral point found on increasing the pressure is always a turning point.

D. Increasing V in experiment I

We first set $V = 0$. Then Z and P are both zero no matter the value of B, and the eigenvalues satisfying Eqs. (18)–(20) are positive and independent of B.

The stable values of B lie in the range $(0,\lambda_1^2)$, and the critical value of B, at $V=0$, is $\lambda_1^2(V=0)$. Then we set B to a value less than $B_{\text{crit}}(V=0)$ and observe that at $V=0$ all the eigenvalues lie to the right of B, i.e., $\lambda_1^2(B,V=0)>B$. Holding B fixed we increase V whereupon the eigenvalues decrease and sooner or later the drop shape becomes unstable at a value of V denoted $V_{\text{crit}}(B)$, *viz.,*

$$\lambda_1^2(B,V_{\text{crit}})=B. \tag{23}$$

Now at any B and V, where we have Z and P, we wish to know if we can increase V. We can if we can solve Eqs. (8)–(10) for $\dot{Z}$. The $\dot{Z}$ problem is not homogeneous, being driven by the right-hand side of Eq. (10). The corresponding homogeneous problem has only the solution $\dot{Z}=0$ so long as B and V are such that $\lambda_1^2(B,V)\neq B$. Thus as V increases at a given B we can find $\dot{Z}$ until V reaches $V_{\text{crit}}(B)$. At that point, where $\lambda_1^2(B,V_{\text{crit}})=B$, a solvability condition, *viz.,*

$$C\iint_{\mathcal{A}}\dot{Z}\,dx\,dy=0 \tag{24}$$

must be satisfied, and it is not satisfied because C is not zero. Thus the drop has become unstable at the greatest value of V, and the increase of V halts at the point of instability. The drop breaks at a turning point, not at a bifurcation point, and the pattern is determined by ψ_1.

E. Increasing P in experiment II

We run experiment II just like experiment I. We first set $P=0$ whence $Z=0$ and $V=0$ for all values of B. At first the eigenvalues are just as they were in experiment I, again independent of B, and the critical value of B, corresponding to a nonzero solution, Z_1, to the perturbation problem, is

$$B=\lambda_1^2(P=0)=\lambda_1^2(V=0).$$

Again we set $B<B_{\text{crit}}(P=0)$ and increase P. At $P=0$ the eigenvalues lie greater than B but as P increases they move toward B and the drop shape becomes critical, i.e., Eqs. (14) and (15) have a solution $Z_1\neq 0$, at a value of P such that

$$\lambda_1^2(B,P)=B.$$

This defines the critical value of P, *viz.,* $P_{\text{crit}}(B)$.

Having a drop shape, Z, at a value of P along the path of increasing P, we wish to know if we can increase P. We can if we can find $\dot{Z}$, i.e., if we can solve Eqs. (16) and (17) for $\dot{Z}$ where $\dot{Z}$ is driven by the inhomogeneity in Eq. (16). The corresponding homogeneous problem has only the solution zero, hence the inhomogeneous problem can be solved for $\dot{Z}$, so long as $\lambda_1^2(B,P)>B$. This obtains until we reach the critical drop shape where $\lambda_1^2(B,P)=B$. At that point a solvability condition must be satisfied, *viz.,*

$$\iint_{\mathcal{A}}\psi_1\,dx\,dy=0,$$

and it is not satisfied because $\iint_{\mathcal{A}}\psi_1\,dx\,dy$ cannot be zero. Thus the drop becomes unstable at the greatest value of P, and the increase of P halts at the point of instability.

III. THE DIFFUSION EIGENVALUE PROBLEM

To see what we can say about drops suspended from arbitrary cross sections, we introduce an eigenvalue problem depending only on $Z(x,y)$ no matter how Z is obtained. It is

$$-\mu^2\phi=\mathcal{L}\phi \tag{25}$$

and

$$\phi = 0 \quad \text{on} \quad \mathcal{C}. \tag{26}$$

This is the eigenvalue problem corresponding to the way Wente [13] thinks about running pressure-controlled experiments. But the Z that appears in $\mathcal{L}$ corresponds to our experiments.

If Z is zero, $\mathcal{L} = \nabla^2$ and Eq. (25) is an ordinary diffusion eigenvalue problem. Otherwise Eq. (25) is a diffusion eigenvalue problem having a space-dependent diffusivity. The base equations corresponding to our experiments differ and so too their eigenvalue problems. Each differs from Eq. (25), yet the solutions to each can be written in terms of the solutions to Eqs. (25) and (26).

Now $\mathcal{L}$ is self-adjoint, and we have

$$\begin{aligned}\iint_{\mathcal{A}} \phi\, \mathcal{L}\, \phi \, dA &= -\iint_{\mathcal{A}} dA \nabla\phi \cdot \frac{\overrightarrow{\overrightarrow{I}}\,(1 + \nabla Z \cdot \nabla Z) - \nabla Z\, \nabla Z}{(1 + \nabla Z \cdot \nabla Z)^{3/2}} \cdot \nabla\phi \\ &= -\iint_{\mathcal{A}} \frac{|\nabla\phi|^2 + |\nabla\phi \times \nabla Z|^2}{(1 + \nabla Z \cdot \nabla Z)^{3/2}}\, dA. \end{aligned} \tag{27}$$

Hence we denote the solutions to Eqs. (25) and (26)

$$0 < \mu_1^2 < \mu_2^2 < \mu_3^2 \cdots$$

and

$$\phi_1 > 0, \quad \phi_2, \phi_3, \ldots,$$

and we denote the integrals of the ϕ by I, *viz.,*

$$I_i = \iint_{\mathcal{A}} \phi_i \, dx\, dy,$$

where $I_1 > 0$.

Our solutions to Eqs. (25) and (26) depend on the drop shape Z where Z gives us what might be called the diffusion coefficient, an input to Eq. (25).

On an arbitrary cross section it is likely that none of the I_i are zero, and, assuming this is so, none of the C in Eq. (18) or the integrals of the eigenfunctions in Eq. (21) can be zero.

We start with experiment I and we solve the eigenvalue problem at constant B and V, *viz.,* Eqs. (18)–(20), by expanding ψ in the eigenfunctions ϕ_i where we assume that $\iint_{\mathcal{A}} \phi_i^2\, dx\, dy = 1$. Thus we have

$$\psi = \sum c_i\, \phi_i, \quad c_i = \iint_{\mathcal{A}} \psi\, \phi_i \, dx\, dy,$$

and we find

$$c_i = \frac{C\, I_i}{\lambda^2 - \mu_i^2},$$

whence ψ is given by

$$\psi = C \sum \frac{I_i}{\lambda^2 - \mu_i^2}\, \phi_i.$$

Thus because $C \neq 0$ and $\iint_{\mathcal{A}} \psi\, dx\, dy = 0$, we can obtain the λ_i by solving

$$\sum \frac{I_i^2}{\lambda^2 - \mu_i^2} = 0. \tag{28}$$

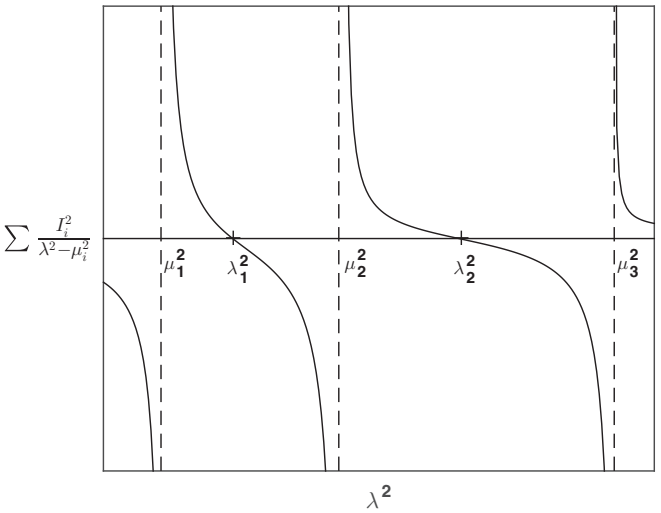

FIG. 3. Graph of Eq. (28).

From the graph of the left-hand side of Eq. (28) versus λ^2, shown in Fig. 3, we derive the ordering

$$0 < \mu_1^2 < \lambda_1^2 < \mu_2^2 < \lambda_2^2 < \cdots,$$

which holds for all B and V.

In the case of experiment II we can solve the eigenvalue problem at constant B and P [Eqs. (21) and (22)] in the same way. But first, because we wish to learn about both experiments, we set the values of B and V and obtain Z and $P^{(\mathrm{I})}$, solutions to the drop shape problem (I). Then we set B at the same value and set $P^{(\mathrm{II})}$ such that $P^{(\mathrm{II})} - B^* \frac{V}{A} = P^{(\mathrm{I})}$ holds. By doing this the shape Z is the same in the two experiments and so too V. Thus the solutions to the diffusion eigenvalue problem [Eqs. (25) and (26)] are common to experiments (I) and (II), and we solve Eqs. (21) and (22) by again expanding ψ in the set of ϕ_i. By doing this we obtain

$$c_i = \frac{I_i}{\lambda^2 - \mu_i^2} B^* \frac{1}{A} \iint_{\mathcal{A}} \psi \, dx \, dy,$$

whence our equation for the λ^2 is now

$$\sum \frac{I_i^2}{\lambda^2 - \mu_i^2} = \frac{1}{B^*}. \tag{29}$$

The left-hand-side of Eq. (29) is plotted versus λ^2 in Fig. 4, and we conclude

$$0 < \mu_1^2 < \left(\lambda_1^2\right)^{(\mathrm{II})} < \left(\lambda_1^2\right)^{(\mathrm{I})} < \mu_2^2 < \left(\lambda_2^2\right)^{(\mathrm{II})} < \left(\lambda_2^2\right)^{(\mathrm{I})} < \mu_3^2 < \cdots. \tag{30}$$

At large values of B^*, $(\lambda_i^2)^{(\mathrm{II})} \longrightarrow (\lambda_i^2)^{(\mathrm{I})}$, at small values of B^*, $(\lambda_i^2)^{(\mathrm{II})} \longrightarrow \mu_i^2$. If we set a value of B, the shapes $z = Z(x, y, B, V)$ or $z = Z(x, y, B, P)$ are stable to small perturbations so long as B is not one of the eigenvalues $(\lambda^2)^{(\mathrm{I})}(B, V)$ or $(\lambda^2)^{(\mathrm{II})}(B, P)$.

We also can see that experiment II is less stable than experiment I. Thus as we increase V in I and P in II we always have the same Z and V, but we know $(\lambda_1^2)^{(\mathrm{II})}(B, P) < (\lambda_1^2)^{(\mathrm{I})}(B, V)$; cf. Figs. 3 and 4. Hence experiment II becomes unstable at a volume and shape at which experiment I is stable. Indeed, the greatest volume in I exceeds the greatest volume in II.

Now B^* is important. If its effect is omitted [2], experiment II always acts like Wente's [13] pressure-controlled experiment, *viz.,* increasing P always ends in a turning point. No bifurcation

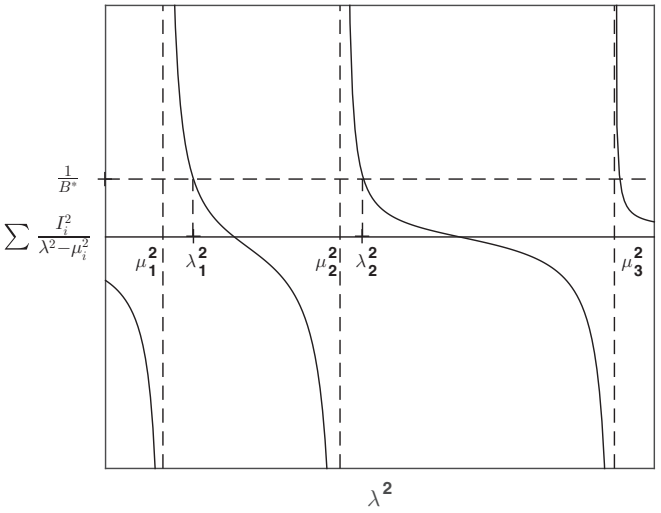

FIG. 4. Graph of Eq. (29).

points can be found. In fact, on omitting B^* the diffusion eigenvalue problem tells us everything about experiment II, and a constant pressure experiment would be predicted to have an instability before it ought to, *viz.*, $\mu_1^2 < \lambda_1^2$, and no bifurcation point can precede the turning point.

Adding symmetry

Now in all of the foregoing we only need $I_1 \neq 0$ and $I_2 \neq 0$ to keep λ_1^2 and λ_2^2 apart, i.e., to keep the fundamental eigenvalue simple, and hence the drop is always unstable to a ψ_1 mode having one internal nodal curve. But if the cross section were a rectangle or an ellipse the symmetry of Z, and hence the symmetry of ϕ_2 ought to cause I_2 to be zero.

Thus if I_2 is zero at any B and V, one of the two smallest solutions, λ^2, ψ, to Eqs. (18)–(20) will be

$$\lambda^2 = \mu_2^2, \quad \psi = \phi_2, \quad \iint_{\mathcal{A}} \psi \, dx \, dy = 0, \quad C = 0.$$

On plotting $\sum_{i=1,3,\ldots} \frac{I_i^2}{\lambda^2-\mu_i^2}$ versus λ^2, omitting the term corresponding to $i = 2$, we find the other solution will be on (μ_1^2, μ_3^2), but we don't know on which side of μ_2^2 it lies. Thus one eigenvalue is pinned at μ_2^2 while the other may lie to its left or right. This is illustrated in Fig. 5. The two eigenfunctions have different symmetries.

Here then is our conclusion: if the cross section has no symmetry, we can increase V to the point of instability and we will see only continuous dependence on B. Upon adding enough symmetry, at some B we will see one pattern at critical, at others another pattern.

IV. SYMMETRIC CROSS SECTIONS

The symmetry of a drop pinned to a curve bounding a symmetric cross section leads to symmetry conditions on the solutions to the diffusion eigenvalue problem. Thus we expect to find cross sections for which $I_2 = \iint_{\mathcal{A}} \phi_2 \, dx \, dy = 0$ and, hence, for which one of the solutions to the eigenvalue problems, Eqs. (18)–(20) and Eqs. (21) and (22), will be

$$\lambda^2 = \mu_2^2, \quad \psi = \phi_2, \quad \text{and} \quad C = 0 = \iint_{\mathcal{A}} \psi \, dx \, dy.$$

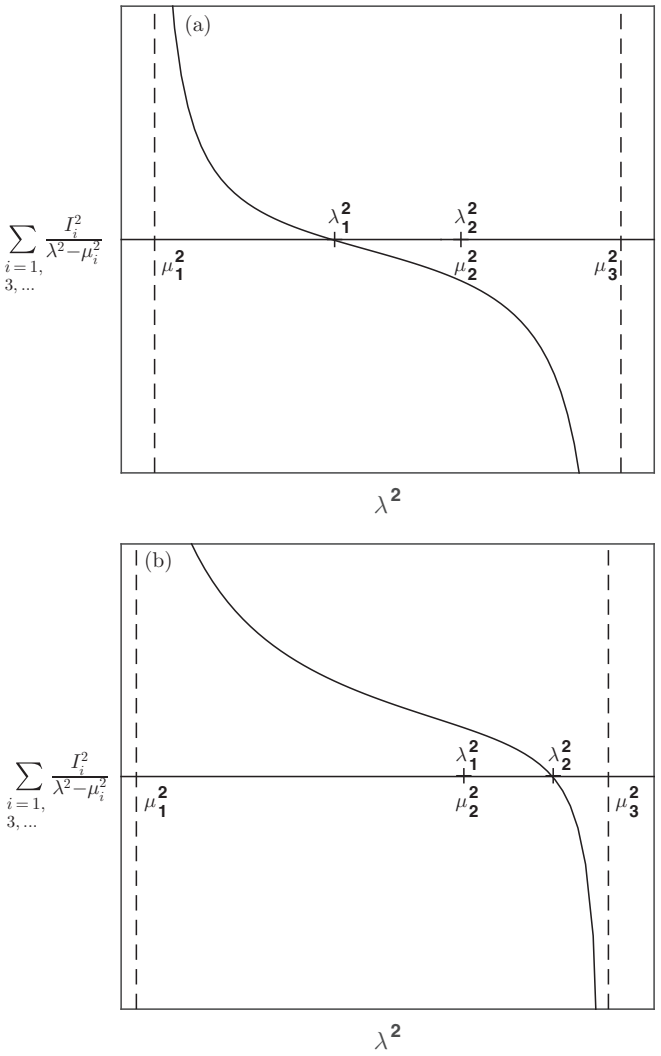

FIG. 5. Graph of Eq. (28) depicting two cases: (a) $\mu_1^2 < \lambda_1^2 < \mu_2^2$, $\lambda_2^2 = \mu_2^2$ and (b) $\lambda_1^2 = \mu_2^2$, $\mu_2^2 < \lambda_2^2$.

The eigenvalues of interest are the smallest and the next smallest, one being equal to μ_2^2, the other lying on the interval (μ_1^2, μ_3^2). The corresponding eigenfunctions have different shapes, and the one accompanying the smallest eigenvalue will predict the pattern at drop breakup.

A. One-dimensional model, experiments I and II

We ought to begin with the case of a circular cross section, but everything of interest for a drop pinned to a circle is already present in a simple one-dimensional model. One dimension, two dimensions, etc., refer to the number of independent variables. In one dimension Z depends only on x, it is independent of y and hence there is only one curvature. At $Z = 0$, and $V = 0$, all of our drop problems are Rayleigh-Taylor problems. They remain Rayleigh-Taylor-like for small increases in V, but for how long depends on B.

Experiment I

We start with the first experiment and with a drop having the shape $Z = Z(x,B,V)$ where Z satisfies

$$P - BZ = \frac{d}{dx}\frac{Z_x}{\left(1+Z_x^2\right)^{1/2}}, \tag{31}$$

$$Z = 0 \quad \text{at} \quad x = \pm 1, \tag{32}$$

and

$$\int_{-1}^{1} Z\,dx = -V. \tag{33}$$

The perturbation problem is

$$P_1 - BZ_1 = \frac{d}{dx}\frac{Z_{1x}}{\left(1+Z_x^2\right)^{3/2}}, \tag{34}$$

$$Z_1 = 0 \quad \text{at} \quad x = \pm 1, \tag{35}$$

and

$$\int_{-1}^{1} Z_1\,dx = 0. \tag{36}$$

The eigenvalue problem is

$$C - \lambda^2\psi = \frac{d}{dx}\frac{\psi_x}{\left(1+Z_x^2\right)^{3/2}}, \tag{37}$$

$$\psi = 0 \quad \text{at} \quad x = \pm 1, \tag{38}$$

and

$$\int_{-1}^{1} \psi\,dx = 0. \tag{39}$$

And the $\dot{Z} = \frac{dZ}{dV}$ problem is

$$\dot{P} - B\dot{Z} = \frac{d}{dx}\frac{\dot{Z}_x}{\left(1+Z_x^2\right)^{3/2}}, \tag{40}$$

$$\dot{Z} = 0 \quad \text{at} \quad x = \pm 1, \tag{41}$$

and

$$\int_{-1}^{1} \dot{Z}\,dx = -1. \tag{42}$$

Now, the drop shape, Z, is an even function of x and thus the solutions to the eigenvalue problem are either odd or even functions of x.

The diffusion eigenvalue problem is

$$\frac{d}{dx}\frac{\phi_x}{\left(1+Z_x^2\right)^{3/2}} + \mu^2\phi = 0 \tag{43}$$

and

$$\phi = 0 \quad \text{at} \quad x = \pm 1, \tag{44}$$

and we denote its solutions by

$$0 < \mu_1^2 < \mu_2^2 < \mu_3^2$$

and

$$\phi_1(\text{even}) > 0, \quad \phi_2(\text{odd}), \quad \phi_3(\text{even}), \ldots, \quad I_1 > 0, \quad I_2 = 0, \quad I_3 \neq 0, \ldots.$$

We first set $V = 0$, hence $Z = 0$, then for any B we have odd and even eigenfunctions, *viz.,*

$$\psi = \sin \lambda x, \quad \lambda^2 = n^2\pi^2, \quad C = 0$$

and

$$\psi = \cos \lambda x - \cos \lambda, \quad \frac{\sin \lambda}{\lambda} - \cos \lambda = 0, \quad C = -\lambda^2 \cos \lambda,$$

whence the least value of λ^2 is π^2, $B_{\text{crit}} = \pi^2$, ψ is odd, and at B_{crit} the drop is unstable to a perturbation having odd symmetry.

Now we set B to a value less than π^2 and increase V from zero. For B near π^2 the fundamental eigenfunction ought to remain odd upon increasing V, and we ought to arrive at the critical value of V where $\lambda^2(B, V_{\text{crit}}) = \mu_2^2(B, V_{\text{crit}}) = B$ is satisfied and where the corresponding eigenfunction is an odd function of x.

We wish to know if V_{crit} limits the increase in V, i.e., we wish to know if Eqs. (40)–(42) have a solution at V_{crit} where $\lambda^2(B, V_{\text{crit}}) = B$. The solvability condition, *viz.,*

$$\int_{-1}^{1} \dot{P}\, \psi \, dx - \int_{-1}^{1} C \dot{Z} \, dx = 0$$

is satisfied due to $\int_{-1}^{1} \psi \, dx = 0 = C$.

Thus our critical point is a bifurcation point, and we can continue to increase V beyond V_{crit}. At V_{crit} we have $\lambda_{\text{odd}}^2(B, V_{\text{crit}}) = B < \lambda_{\text{even}}^2(B, V_{\text{crit}})$. As we increase V, beyond V_{crit}, we have $\lambda_{\text{odd}}^2 = \mu_2^2$ and $\lambda_{\text{even}}^2 \in (\mu_2^2, \mu_3^2)$ both moving to the left and sooner or later $\lambda_{\text{even}}^2(B, V) = B$. Again Eqs. (40)–(42) have a nonzero solution. We have arrived at a second critical point, but now ψ is an even function of x and C is not zero. Hence Eqs. (40)–(42) cannot be solved for $\dot{Z}$ because solvability fails, *viz.,*

$$\int_{-1}^{+1} \dot{P}\, \psi \, dx - \int_{-1}^{+1} C \dot{Z} \, dx = C \neq 0.$$

Thus we have reached the greatest value of V and the second critical point is not a bifurcation point but a turning point. The drop is unstable at the first critical point and presumably breaks in the pattern of an odd eigenfunction, so any advance through this point is hypothetical and we see that the drop does not break at the greatest volume.

We present what we have found in a series of figures where we denote the first two eigenvalues λ_{odd}^2 and λ_{even}^2 because the order $\lambda_{\text{odd}}^2 < \lambda_{\text{even}}^2$ is not maintained as B decreases. We plot V versus P at a sequence of B, and at each B we indicate the eigenvalues $\mu_1^2, \mu_2^2, \mu_3^2, \lambda_{\text{odd}}^2$ and λ_{even}^2 at each of a set of V.

First at B slightly less than π^2, we present Fig. 6(a), where we see the eigenvalues moving to the left as V increases. The bifurcation point and the turning point are marked. Figure 6(b) is drawn at a lower value of B and shows the bifurcation point moving closer to the turning point. Decreasing B again we arrive at Fig. 7, where $\lambda_{\text{odd}}^2 = B = \lambda_{\text{even}}^2$. The corresponding value of B is denoted $B_\star$.

For all $B < B_\star$, λ_{even}^2 is less than λ_{odd}^2 at critical. Now, no matter the value of B, at $V = 0$ we have $\lambda_{\text{odd}}^2 < \lambda_{\text{even}}^2$. At $B = B_\star$, the exchange of the order occurs at the critical value of V. For $B < B_\star$ the change in the order occurs at $0 < V < V_{\text{crit}}$ and we have Fig. 8.

Thus there is a value of B, denoted $B_\star$, at which, at critical, the fundamental eigenvalue is a double root. For larger values of B the first critical point is a bifurcation point corresponding to an odd eigenfunction, for smaller values of B the first critical point is a turning point corresponding to

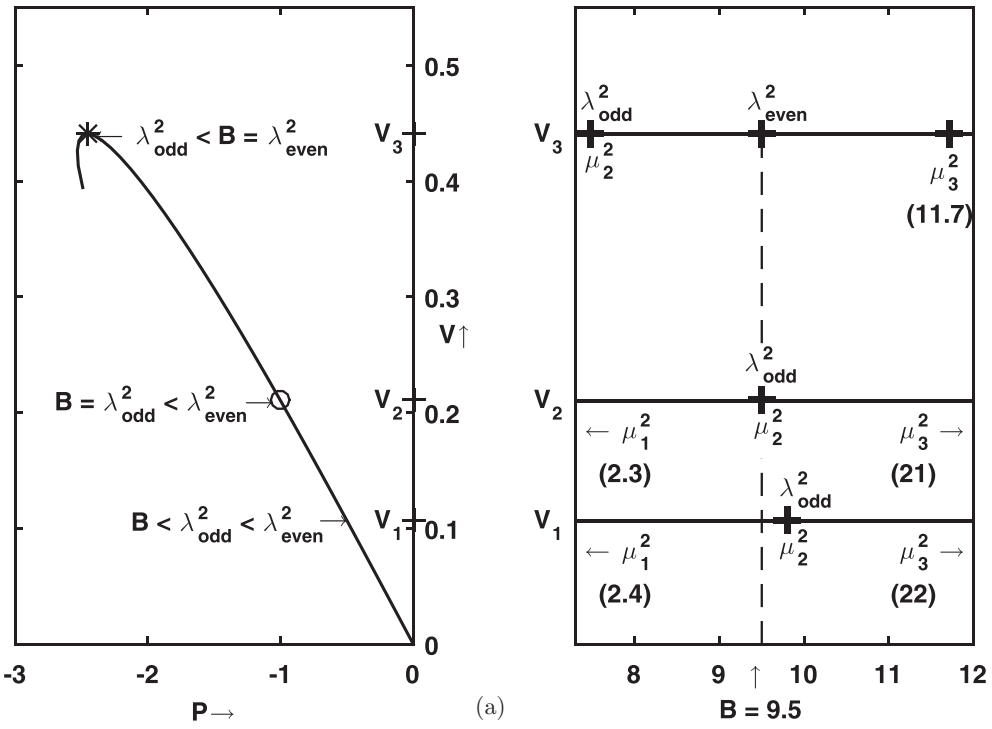

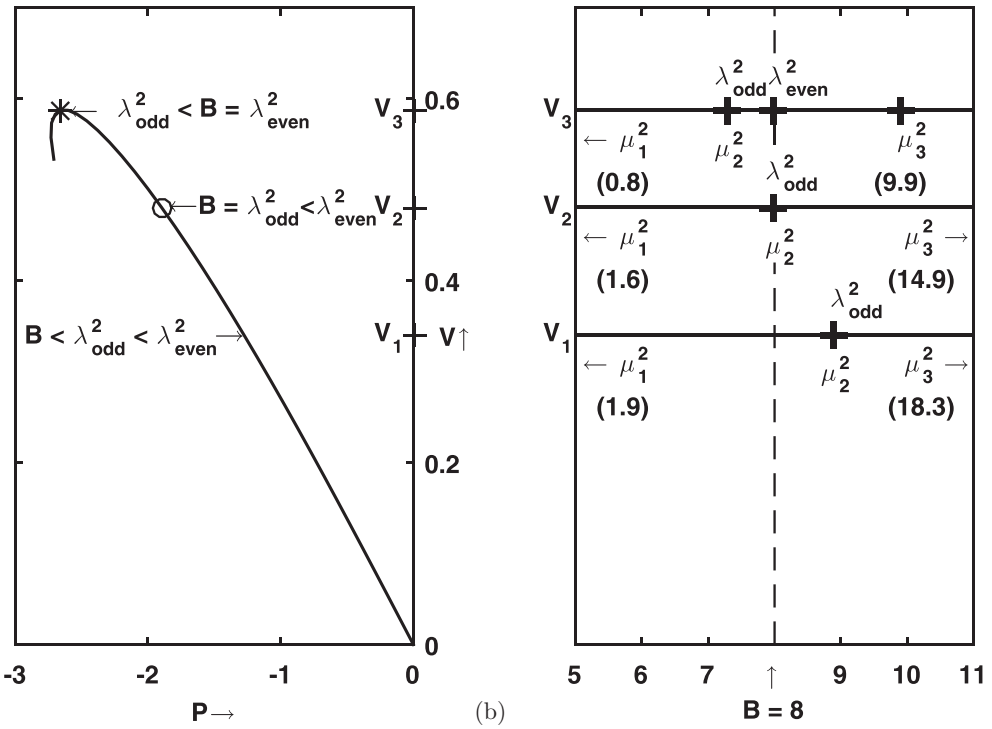

FIG. 6. Graph of V vs P depicting λ^2: (a) $B = 9.5$, (b) $B = 8$; o = bifurcation point, $*$ = turning point.

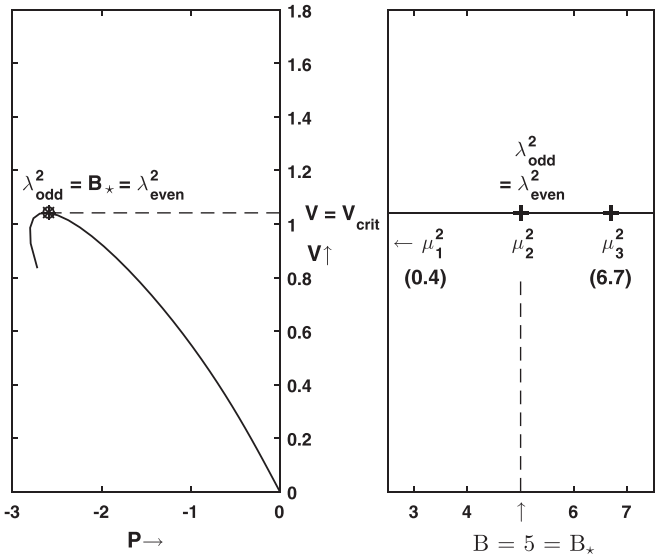

FIG. 7. Graph of V vs P at $B = B_\star = 5$; o = bifurcation point, $*$ = turning point.

an even eigenfunction. The pattern of the instability changes as we decrease B from large values to small values.

B. Finding a bifurcation point without solving an eigenvalue problem

Ordinarily, critical points are found by solving eigenvalue problems. But, because the drop is static, we can derive an exceptional result. Thus, given a base curve V versus P, we can find bifurcation points along the curve by drawing a line which intersects the curve. In this section we derive and illustrate this result.

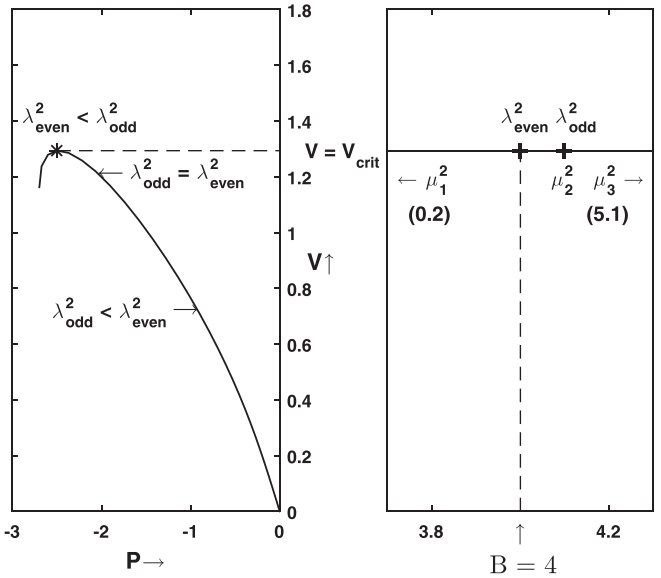

FIG. 8. Graph of V vs P at $B < B_\star$, $B = 4$; $*$ = turning point.

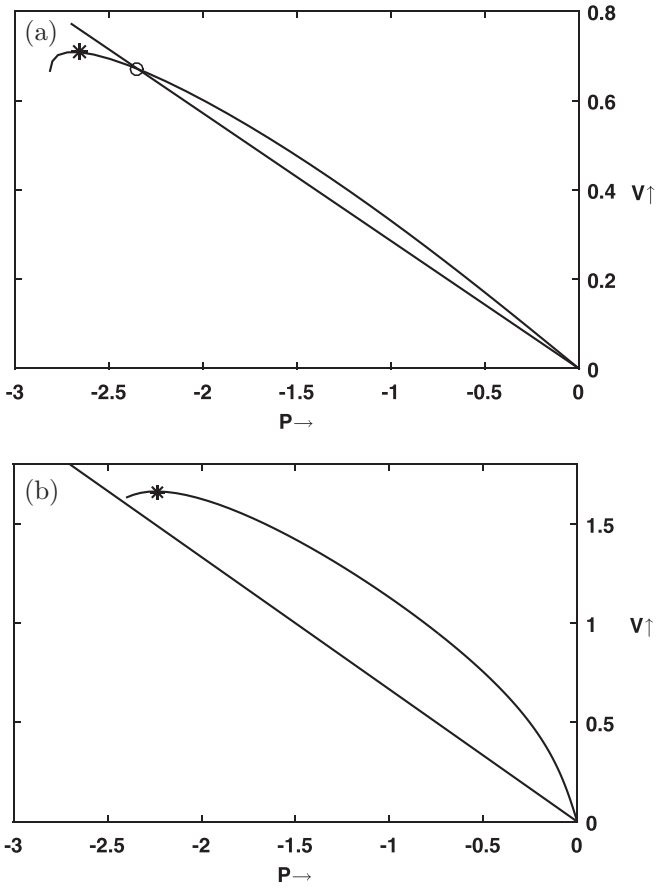

FIG. 9. Graphs showing the intersection of $2P + BV = 0$ and V vs P: (a) large B, (b) small B; o = bifurcation point, $*$ = turning point.

Upon integrating Eq. (31) over $-1 \leqslant x \leqslant 1$ we have

$$2P + BV = \frac{Z_x}{\left(1 + Z_x^2\right)^{1/2}}\Bigg|_{x=-1}^{x=1}. \tag{45}$$

The right-hand side is the vertical force that the pins exert on the drop; see Appendix C.

For input values of B and V we solve Eqs. (31)–(33) for Z and P and plot the curve V versus P. Now we will see that the right-hand side of Eq. (45) is zero at a bifurcation point. Hence the line $2P + BV = 0$ intersects the curve V versus P at the first critical point, if the critical point is a bifurcation point. This is illustrated in Figs. 9(a) and 9(b), which present the construction for two values of B, one above $B_\star$, and the other below.

To see that the right-hand side of Eq. (45) is zero at a bifurcation point and thus to see that we can find a bifurcation point using only the base shape, we need the equation for Z_x. Differentiating Eq. (31) we have

$$-BZ_x = \frac{d}{dx}\frac{(Z_x)_x}{\left(1 + Z_x^2\right)^{3/2}}, \tag{46}$$

and we also have, due to pinned edges,

$$\int_{-1}^{+1} Z_x \, dx = 0.$$

At a critical point corresponding to an odd eigenfunction we have $C = 0$ in Eq. (37). Multiplying Eq. (37) by Z_x, Eq. (46) by ψ, subtracting, integrating over $-1 \leqslant x \leqslant 1$, using $\lambda^2 = B$, Z even, and Z_x odd we have

$$0 = \frac{2Z_x(x=1)}{\left[1 + Z_x^2(x=1)\right]^{3/2}}$$

due to the fact that ψ_x, even, cannot be zero at $x = \pm 1$. Thus we conclude: Z_x is zero at $x = \pm 1$ at a bifurcation point, and hence the right-hand side of Eq. (45) is zero. This is due, not only to symmetry, but also to the fact that the ends are pinned. The upward force exerted by the pins on the drop vanishes at the bifurcation point [9].

Experiment II

In the case of experiment II where B and P are the inputs and Z and V the outputs, Z satisfies

$$P + B^* \frac{1}{2} \int_{-1}^{1} Z \, dx - BZ = \frac{d}{dx} \frac{Z_x}{\left(1 + Z_x^2\right)^{1/2}}, \quad Z = 0 \quad \text{at} \quad x = \pm 1. \tag{47}$$

This is our one-dimensional model, and we must have $B < B^*$.

We solve Eq. (47) by first solving Eqs. (31)–(33) for Z and $P^{(\mathrm{I})}$ given B and V. Then if we set $P^{(\mathrm{II})}$ in Eq. (47) to $P^{(\mathrm{I})} + \frac{1}{2} B^* V$, Z and V satisfying Eq. (47) are identical to Z and V satisfying Eqs. (31)–(33), and hence we can derive the V versus P curve in experiment II from the V versus P curve in experiment I.

At $P = 0$, hence $Z = 0$ and $V = 0$, the solutions to the eigenvalue problem, Eqs. (21) and (22), are

$$\psi = \sin \lambda x, \quad \lambda^2 = n^2 \pi^2, \quad \int_{-1}^{1} \psi \, dx = 0$$

and

$$\psi = \cos \lambda x + \frac{B^*/\lambda^2}{1 - \frac{B^*}{\lambda^2}} \frac{1}{\lambda} \sin \lambda, \quad 1 - \frac{\lambda^2}{B^*} = \frac{\sin \lambda}{\lambda \cos \lambda}, \quad \int_{-1}^{+1} \psi \, dx = \frac{2 \sin \lambda}{\lambda} \frac{1}{1 - \frac{\lambda^2}{B^*}},$$

and we have $\mu_1^2 = \frac{1}{4}\pi^2$, $\mu_2^2 = \pi^2$, ...

We are looking for the smallest λ^2 because at $P = 0$ this is B_{crit}.

If $B^* < \pi^2$ then the first eigenfunction is even the second odd and $B^* < \lambda_1^2 < \pi^2 = \lambda_2^2$. But if $B^* > \pi^2$ the first eigenfunction is odd, the second even, and we have $\lambda_1^2 = \pi^2 < \lambda_2^2 < B^*$.

Now we must have $B < B^*$, and thus at $P = 0$, if B^* is less than π^2, there are no values of λ^2 that can be equal to B, and we have stability to all small perturbations.

If B^* is greater than π^2, the critical value of B at $P = 0$ is π^2. Thus we can set a value of B less than π^2 and increase P. Now the drop shapes and volumes in the second experiment derive from those in the first experiment, and we obtain the curves shown in Fig. 10.

Experiment II also has a straight line construction predicting the bifurcation point using only the base shape:

$$2P^{(\mathrm{II})} - B^* V + BV = 0, \tag{48}$$

and it predicts the bifurcation point shown in the figure.

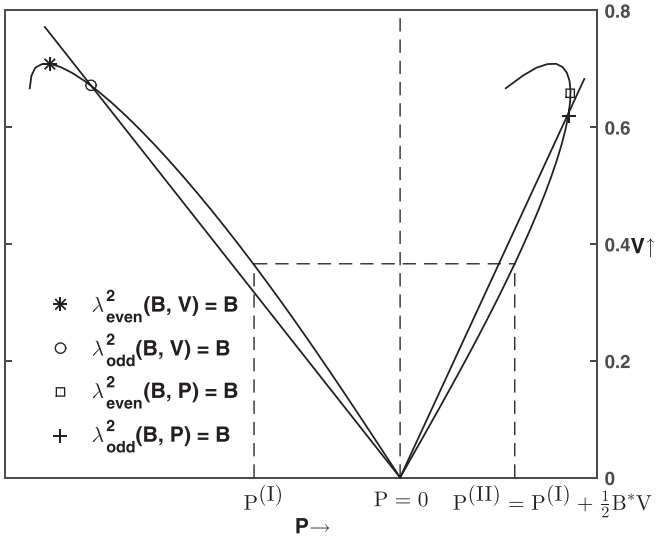

FIG. 10. Graphs of V vs P showing that experiment II is less stable than experiment I; $B = 7$, $B^* = \frac{11}{10}\pi^2$.

The figure also indicates that perturbations at constant V are stable at higher V than perturbations at constant P. Of course this repeats what we learned for arbitrary cross sections.

There is a value of B, denoted $B_\star^{(\mathrm{II})}$, such that $\lambda^2_{\mathrm{odd}}(B_\star^{(\mathrm{II})}) = \lambda^2_{\mathrm{even}}(B_\star^{(\mathrm{II})})$. Its significance is the same as that of $B_\star$ in experiment I, *viz.*, $B_\star^{(\mathrm{I})}$. Now $B_\star^{(\mathrm{II})}$ depends on B^* and as B^* becomes large $B_\star^{(\mathrm{II})} \to B_\star^{(\mathrm{I})}$ because $\lambda^{2\,(\mathrm{II})} \to \lambda^{2\,(\mathrm{I})}$; see Fig. 4. In Fig. 10 we have $B > B_\star^{(\mathrm{II})}$.

C. Square and rectangular cross sections, Experiment I

Both rectangular and square cross sections have enough symmetry for I_2 to vanish and hence we wish to see if our way of locating bifurcation points, using only the shape of the drop, carries over to these cross sections, one having more symmetry than the other.

Denote the cross section by $\mathcal{A}$. It is bounded by a curve $\mathcal{C}$ along which $Z = 0$ and the normal to $\mathcal{C}$ in the plane of $\mathcal{A}$ is

$$\frac{\nabla Z}{(\nabla Z \cdot \nabla Z)^{1/2}}.$$

Thus, integrating Eq. (1) over the cross section we have

$$PA + BV = \int_{\mathcal{C}} ds\, \frac{(\nabla Z \cdot \nabla Z)^{1/2}}{(1 + \nabla Z \cdot \nabla Z)^{1/2}}, \tag{49}$$

where the right-hand side is zero if and only if ∇Z is pointwise zero.

If the cross section is the rectangle $-a \leqslant x \leqslant a$, $-b \leqslant y \leqslant b$, the $C = 0$ solutions to the eigenvalue problem, Eqs. (18)–(20), at $V = 0$ are [5]

$$\sin m\pi \frac{x}{a}\ \sin n\pi \frac{y}{b} \quad m, \quad n = 1,2,\ldots,$$
$$\sin m\pi \frac{x}{a}\ \cos\left(n + \frac{1}{2}\right)\pi \frac{y}{b}, \quad m = 1,2,\ldots \quad n = 0,1,\ldots,$$

and

$$\cos\left(m+\frac{1}{2}\right)\pi\frac{x}{a}\ \sin n\pi\frac{y}{a},\quad m=0,1,\ldots\quad n=1,2,\ldots.$$

And, if $a>b$, the least λ^2 corresponds to

$$\cos\frac{1}{2}\pi\frac{x}{a}\sin\pi\ \frac{y}{b},$$

even in x, odd in y. There are solutions where $C\neq 0$ but the corresponding eigenvalues are greater than $\frac{1}{4}\frac{\pi^2}{a^2}+\frac{\pi^2}{b^2}$.

We assume the symmetry of the eigenfunctions at $V>0$ is the same as it is at $V=0$, and we set B and advance V until we arrive at the bifurcation point where $\lambda_1^2(B,V)=B$ and where λ_1^2 and ψ_1 satisfy

$$-\lambda_1^2\psi_1=\mathcal{L}\psi_1,\quad C_1=0. \tag{50}$$

Now, we differentiate Eq. (1) with respect to y obtaining

$$-BZ_y=\mathcal{L}Z_y, \tag{51}$$

whereupon multiplying Eq. (50) by Z_y, Eq. (51) by ψ_1, subtracting, using $\lambda_1^2=B$ and integrating over $\mathcal{A}$ we have

$$0=\int_{\mathcal{C}}ds\ Z_y\ \frac{\overrightarrow{n}\cdot\nabla\psi}{(1+\nabla Z\cdot\nabla Z)^{3/2}} \tag{52}$$

due to $\overrightarrow{n}=\frac{\nabla Z}{|\nabla Z|}$

Now along $x=\pm a$ we have $Z=0$, hence $Z_y=0$. Along $y=-b$ we have $ds=dx$ and $\overrightarrow{n}\cdot\nabla\psi=-\psi_y$. Along $y=b$ we have $ds=-dx$ and $\overrightarrow{n}\cdot\nabla\psi=\psi_y$. Thus Eq. (52) becomes

$$0=\int_{-a}^{a}dx\ \frac{Z_y(-\psi_y)}{\left(1+Z_y^2\right)^{3/2}}-\int_{a}^{-a}dx\ \frac{Z_y(\psi_y)}{\left(1+Z_y^2\right)^{3/2}}. \tag{53}$$

The first integral is along $y=-b$, the second is along $y=b$. Now Z is an even function of y and hence Z_y is an odd function of y, *viz.*, $Z_y(x,-b)=-Z_y(x,b)$. Because ψ is an odd function of y we have $\psi_y(x,-b)=+\psi_y(x,b)$ and ψ_y is not zero because $\psi(x,-b)=0=\psi(x,b)$. Thus, by Eq. (53) we have $Z_y=0$ on $\mathcal{C}$ at a bifurcation point.

However, there is nothing we can say about Z_x on $\mathcal{C}$, and hence not enough about ∇Z on $\mathcal{C}$ in the case of a rectangular cross section.

But for a square cross section the least eigenvalue at $C=0$ corresponds to two eigenfunctions, one odd in x, even in y, the other even in x, odd in y. Thus we can carry out the above derivation twice at the same eigenvalue equal to B and conclude that ∇Z vanishes on $\mathcal{C}$ at a bifurcation point.

Hence, in the case of a square cross section, we can plot V versus P and its intersection with $PA+BV=0$ will locate the critical point so long as it is a bifurcation point, all without using more than the base solution. The base solution also identifies the turning point.

D. Circular cross section Experiment I

On a circular cross section, where our inputs are B and V and our outputs are $Z(r)$ and P, Eqs. (1)–(9) are, first,

$$P-BZ=\frac{1}{r}\frac{d}{dr}\ \frac{r}{\left(1+Z_r^2\right)^{1/2}}\frac{dZ}{dr}, \tag{54}$$

$$Z=0\quad\text{at}\quad r=1, \tag{55}$$

and

$$-2\pi \int_0^1 Zr\,dr = V; \tag{56}$$

second,

$$\dot{P} - B\,\dot{Z} = \frac{1}{r}\frac{d}{dr}\frac{r}{\left(1+Z_r^2\right)^{3/2}}\frac{d\,\dot{Z}}{dr}, \tag{57}$$

$$\dot{Z} = 0 \quad \text{at} \quad r = 1, \tag{58}$$

and

$$-2\pi \int_0^1 \dot{Z}\,r\,dr = 1; \tag{59}$$

and, third,

$$C - \lambda^2\psi = \frac{1}{r}\frac{\partial}{\partial r}\frac{r}{\left(1+Z_r^2\right)^{3/2}}\frac{\partial\psi}{\partial r} + \frac{1}{\left(1+Z_r^2\right)^{1/2}}\frac{1}{r^2}\frac{\partial^2\psi}{\partial\theta^2}, \tag{60}$$

$$\psi = 0 \quad \text{at} \quad r = 1, \tag{61}$$

and

$$\int_0^{2\pi} d\theta \int_0^1 \psi r\,dr = 0, \tag{62}$$

where $Z(r)$ in Eqs. (57)–(62) is the solution of Eqs. (54)–(56). If Z is zero, this is the Rayleigh-Taylor problem on a circle, solved by Maxwell [5]. Our aim is to show that everything found out here can be forecast by what we already know about the one-dimensional problem.

We set $V = 0$ whereupon $Z = 0 = P$ for all B. The solutions to Eqs. (60)–(62) are then

$m = 0$:

$$\psi = J_0(\lambda r) - J_0(\lambda), \quad \lambda J_0(\lambda) + 2J_1(\lambda) = 0, \quad C = \lambda^2 J_0(\lambda),$$

$m = 1$:

$$\psi = J_1(\lambda r)\cos\theta, \quad J_1(\lambda) = 0, \quad C = 0.$$

The critical value of B at $V = 0$ is the square of the first positive zero of J_1 and the drop is unstable to a $\cos\theta$ perturbation.

We set $B < B_{\text{crit}}(V = 0)$ and advance V from zero until the least $\lambda^2(B,V)$ attains the value B, *viz.,*

$$\lambda^2(B, V_{\text{crit}}) = B.$$

If B is near $B_{\text{crit}}(V = 0)$, the first critical point corresponds to $m = 1$. It is a bifurcation point and Eqs. (57)–(59) have a solution there. Ideally we can pass through this point and increase V beyond $V_{\text{crit}}(B)$. Doing this we arrive at a point where the least eigenvalue, corresponding now to an $m = 0$ eigenfunction, becomes equal to B. Equations (57)–(59) fail to have a solution, and we have reached the greatest value of V. The instability occurs before V reaches its greatest value.

At a smaller value of B the picture is just as it was in the one-dimensional model, and we come to a value of B where at $V_{\text{crit}}(B)$ the least eigenvalues at $m = 0$ and $m = 1$ coincide and we have

$$\lambda^2(m = 1) = B_\star = \lambda^2(m = 0).$$

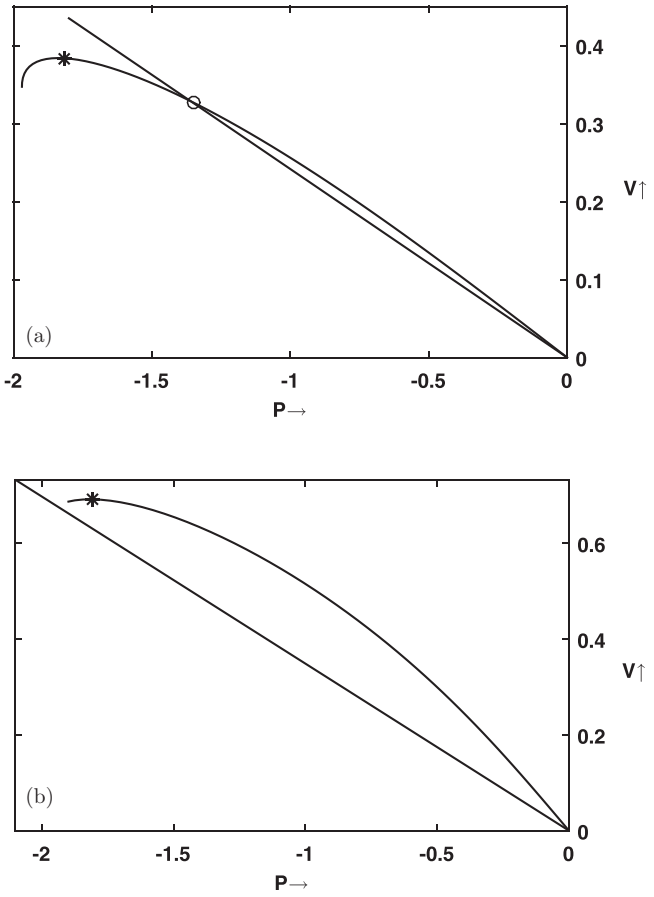

FIG. 11. The V vs P curve for a circular cross section showing the straight line construction; $B = 13$ (a), B = 9 (b), $B_\star = 10$; o = bifurcation point, $*$ = turning point.

This is the greatest V at that B and it is not preceded by a bifurcation point. For lower values of B the critical V always corresponds to an $m = 0$ eigenfunction, the critical point is a turning point and V_{crit} is the greatest value of V.

There is no qualitative difference between the one-dimensional model and the drop pinned to the edge of a circular cross section. The $m = 1$ eigenfunctions here correspond to the odd eigenfunctions there, the $m = 0$ eigenfunctions to the even eigenfunctions.

Now so long as the drop is critical at an $m = 1$ eigenvalue we can locate the critical point by drawing the line, $P\pi + BV = 0$; see Fig. 11.

To do this we only need to observe that

$$Z_r(r = 1) = 0$$

at critical. Thus, differentiating Eq. (54) with respect to r we have

$$-BZ_r = \frac{1}{r}\frac{d}{dr}\frac{r}{\left(1 + Z_r^2\right)^{3/2}}\frac{dZ_r}{dr} - \frac{1}{\left(1 + Z_r^2\right)^{1/2}}\frac{1}{r^2}Z_r,$$

and observing that the radial part of the $m = 1$ eigenfunction satisfies

$$-\lambda^2\psi = \frac{1}{r}\frac{d}{dr}\frac{r}{\left(1+Z_r^2\right)^{3/2}}\frac{d\psi}{dr} - \frac{1}{\left(1+Z_r^2\right)^{1/2}}\frac{1}{r^2}\psi,$$

we set $\lambda^2 = B$ and derive

$$0 = -\frac{Z_r}{\left(1+Z_r^2\right)^{3/2}}\, r\,\psi_r\Big|_{r=0}^{r=1}, \tag{63}$$

whereupon we have

$$Z_r(r=1) = 0 \tag{64}$$

at critical due to $\psi_r(r=1) \neq 0$. Hence if we multiply Eq. (54) by r and integrate over $0 \leqslant r \leqslant 1$ we obtain

$$P\pi + BV = 0, \tag{65}$$

and we can predict bifurcation points by our familiar construction.

At large values of B the drop breaks before it reaches its greatest volume, and it breaks in an antisymmetric pattern, $m = 1$. At small values of B the drop breaks at its greatest volume, and it breaks in a symmetric pattern, $m = 0$. Now the drop has two curvatures, and it might be thought that the transition from $m = 1$ breakup to $m = 0$ breakup must be due to the transverse curvature asserting itself as it does in a jet or bridge. But that cannot be true because the same transition occurred in the one-dimensional model wherein there is only one curvature. This is a static result. Beyond critical, transverse curvature is dominates the dynamics of breakup [14].

If we view circular and elliptical cross sections in the light of what we know about square and rectangular cross sections we would guess that our straight line construction ought to fail in the case of an ellipse. But what about a cross section in the shape of a ring, $\beta \leqslant r \leqslant 1$? The calculation resulting in Eq. (63) now gives us

$$0 = r\frac{Z_r}{\left(1+Z_r^2\right)^{3/2}}\,\psi_r\Big|_{r=\beta}^{r=1}, \tag{66}$$

where neither $\psi_r(r=1)$ nor $\psi_r(r=\beta)$ is zero. We might wish to conclude $Z_r = 0$ on $\mathcal{C}$ at critical, but it is not true. Equation (66) has solutions other than $Z_r = 0$. We do not have the symmetry needed to conclude $PA + BV = 0$ at critical.

E. A circle displaced to a nearby ellipse of the same cross-sectional area

We are going to set the value of B high enough that a drop pinned to a circle has a bifurcation point at a volume V_0 where the least λ_0^2 is equal to B. Then Z_0, P_0, ψ_0, λ_0^2, and C_0 satisfy Eqs. (54)–(56) and (60)–(62) where $C_0 = 0$, where ψ_0 is an $m = 1$ eigenfunction and where

$$\frac{dZ_0}{dr} = 0 \quad \text{at} \quad r = R_0 = 1.$$

Now we displace the circle to an ellipse of the same cross sectional area and write

$$R(\theta) = R_0 + \varepsilon R_1(\theta),$$

where $R_1(\theta) = R_0\cos 2\theta$

We set B and V to their circle values and look for the corrections Z_1, P_1, ψ_1, and λ_1^2 to Z_0, P_0, ψ_0, and λ_0^2. We find that Z_1 and P_1 must satisfy

$$P_1 - BZ_1 = \mathcal{L}(Z_0)Z_1, \quad Z_1 = 0 \quad \text{at} \quad r = R_0,$$

and

$$\int_0^{2\pi} d\theta \int_0^{R_0} Z_1 r\, dr = 0$$

due to $\frac{dZ_0}{dr} = 0$ at $r = R_0$. Because $B = \lambda_0^2$ we find $Z_1 = A\psi_0$ and $P_1 = 0$.

Now the ellipse has enough symmetry that we can assume its instability at B and V_0, like that of the nearby circle, is a bifurcation point. Thus the equation satisfied by λ_1^2 and ψ_1 is

$$C_1 - \lambda_1^2\psi_0 - \lambda_0^2\psi_1 = \lim_{\varepsilon\to 0} \frac{1}{\varepsilon}\{\mathcal{L}(Z_0 + \varepsilon Z_1)(\psi_0 + \varepsilon\psi_1) - \mathcal{L}(Z_0)\psi_0\},$$

where

$$\mathcal{L}(Z_0 + \varepsilon Z_1) = \mathcal{L}(Z_0) + \varepsilon\, \mathcal{L}(Z_0, Z_1)$$

and where

$$\mathcal{L}(Z_0, Z_1) = \nabla \cdot \left\{ \left(\overrightarrow{\overrightarrow{I}}(1 + \nabla Z_0 \cdot \nabla Z_0) - \nabla Z_0\, \nabla Z_0\right)\left(\frac{-3\nabla Z_0 \cdot \nabla Z_1}{(1 + \nabla Z_0 \cdot \nabla Z_0)^{3/2}}\right) + \frac{\overrightarrow{\overrightarrow{I}}\, 2\nabla Z_0 \cdot \nabla Z_0 - \nabla Z_0\, \nabla Z_1 - \nabla Z_1\, \nabla Z_0}{(1 + \nabla Z_0 \cdot \nabla Z_0)^{5/2}} \right\} \cdot \nabla,$$

whereupon we have

$$C_1 - \lambda_1^2\psi_0 - \lambda_0^2\psi_1 = \mathcal{L}(Z_0)\psi_1 + \mathcal{L}(Z_0, Z_1)\psi_0, \quad \psi_1 = -R_1\frac{\partial\psi_0}{\partial r} \quad \text{at} \quad r = R_0, \tag{67}$$

and

$$\int_0^{2\pi} d\theta \int_0^{R_0} \psi_1 r\, dr = 0.$$

Multiplying Eq. (67) by ψ_0, Eq. (60) by ψ_1, subtracting and integrating over $0 \leqslant \theta \leqslant 2\pi, 0 \leqslant r \leqslant R_0$ we have

$$-\lambda_1^2 \iint_{\mathcal{A}_0} \psi_0^2 r\, dr d\theta = \iint_{\mathcal{A}_0} \{\psi_0\mathcal{L}(Z_0)\psi_1 - \psi_1\mathcal{L}(Z_0)\psi_0\} r\, dr\, d\theta + \iint_{\mathcal{A}_0} \psi_0\mathcal{L}(Z_0, Z_1)\psi_0 r\, dr\, d\theta,$$

where, due to $\nabla Z_0 = \overrightarrow{0}$ on $\mathcal{C}_0$, the first integral on the right-hand side is

$$R_0 \int_0^{2\pi} d\theta\, R_1\left(\frac{\partial\psi_0}{\partial r}\right)^2 (r = R_0) = R_0^2\left[\frac{d\psi_0}{dr}(r = R_0)\right]^2 \int_0^{2\pi} \cos 2\theta\, \cos^2\theta\, d\theta.$$

The second integral on the right-hand side is zero because

$$\int_0^{2\pi} d\theta \cos\theta, \quad \int_0^{2\pi} d\theta \cos^3\theta, \quad \text{and} \quad \int_0^{2\pi} d\theta \cos\theta\, \sin^2\theta$$

all vanish.

Thus λ_1^2 is negative, and hence upon advancing V, λ^2 (ellipse) becomes equal to B before λ^2 (circle) and thus a drop pinned to an ellipse is more unstable than a drop pinned to a circle, the cross-sectional areas being the same.

Now we would guess that if the term $R_1(\theta)$ in the expansion of $R(\theta)$ had terms in $\cos 3\theta$, $\cos 4\theta$, etc., the above would continue to hold true, and hence our straight line construction based on the circle would tell us that most nearby shapes had already reached their first point of instability.

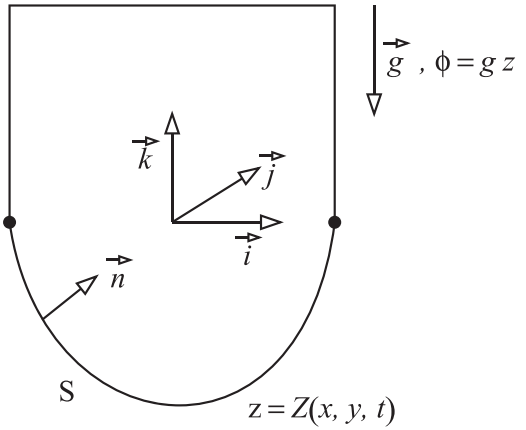

FIG. 12. A sketch of experiment I.

This may not be surprising in view of the fact that the $m = 0$ eigenvalues of ∇^2 on a circle increase if the circle is displaced to a nearby ellipse, the $m = 1$ eigenvalues decrease.

V. CONCLUSIONS

In our study of the stability of a static pendent drop we draw two major conclusions. Both have to do with integral constraints in the problem determining the shape of the drop. The first is that the critical point of the static drop, whether it is formed by volume or pressure control, is bounded and the bound is determined by an eigenvalue problem free of any integral and therefore of any constraint. This is so no matter the symmetry of the curve of the attachment as long as the drop is pinned. The unrestricted eigenvalue problem is termed the diffusion eigenvalue problem, and it corresponds to an ideal thought experiment on static drop formation. This implies that the stability limits for one static drop experiment may be used to bound and even predict the stability limits for drop experiments with other types of control.

The second conclusion applies to experiments where the curve of attachment is made perfectly symmetric. Here we derive a simple construction, knowing only the base drop shape, to determine whether the drop is unsymmetrically or symmetrically unstable. This construction then yields the critical points for either type of instability.

ACKNOWLEDGMENT

Support for X.L. from NSF Grants No. 0968313 and No. 1640677 is acknowledged.

APPENDIX A: NEED THE PERTURBATION BE OTHER THAN HYDROSTATIC AT CRITICAL?

Figure 12 shows a simplified picture of experiment I. There is no light fluid.

Our aim is to show that at critical we have only a hydrostatic solution to the small perturbation problem at constant volume.

Denoting the surface of the drop $z = Z(x,y,t)$, our unscaled nonlinear equations on the domain are

$$\rho \frac{\partial \vec{v}}{\partial t} + \rho \vec{v} \cdot \nabla \vec{v} = \nabla \cdot \vec{\vec{T}} - \rho \nabla \phi$$

and

$$\nabla \cdot \vec{v} = 0.$$

At all walls we have $\vec{n} \cdot \vec{v} = 0$. Along $z = Z(x,y,t)$ we have

$$\vec{n} \cdot \vec{v} = \frac{Z_t}{(1 + \nabla Z \cdot \nabla Z)^{1/2}},$$
$$\vec{n}\,\vec{n} : \vec{\vec{T}} + \gamma 2H = 0,$$

and

$$\vec{t}\,\vec{n} : \vec{\vec{T}} = 0, \quad \text{any tangent } \vec{t},$$

where

$$\vec{n} = \frac{\vec{k} - \nabla Z}{(1 + \nabla Z \cdot \nabla Z)^{1/2}}, \quad \vec{k} \cdot \nabla Z = 0.$$

Assuming we have a base solution to the nonlinear equations, *viz.,*

$$Z = Z_0(x,y), \quad \vec{v}_0 = \vec{0}, \quad \frac{dp_0}{dz} = -\rho g, \quad p_0 = -\rho g z + \text{const},$$

and

$$\vec{\vec{T}} = -p_0 \vec{\vec{I}},$$

we introduce a small perturbation. Thus we write

$$Z = Z_0 + \varepsilon Z_1 \quad \text{and} \quad \vec{v} = \varepsilon \vec{v}_1,$$

and we have

$$\vec{n} = \vec{n}_0 + \varepsilon \vec{n}_1,$$

where

$$\vec{n}_0 = \frac{\vec{k} - \nabla Z_0}{(1 + \nabla Z_0 \cdot \nabla Z_0)^{1/2}}$$

and

$$\vec{n}_1 = -\frac{\vec{\vec{I}}\,(1 + \nabla Z_0 \cdot \nabla Z_0) + (\vec{k} - \nabla Z_0)\nabla Z_0}{(1 + \nabla Z_0 \cdot \nabla Z_0)^{3/2}} \cdot \nabla Z_1.$$

The perturbation problem must be solved on the base domain, the domain obtained by writing $z = Z_0(x,y)$ in place of $z = Z(x,y,t)$ in Fig. 12.

Along $z = Z_0(x,y)$ we have

$$\vec{n}_0\vec{n}_0 : \vec{\vec{T}}_1 + \rho g Z_1 + \gamma 2H_1 = 0, \tag{A1}$$

$$\vec{t}_0\vec{n}_0 : \vec{\vec{T}}_1 = 0, \tag{A2}$$

and

$$\vec{n}_0 \cdot \vec{v}_1 = \frac{Z_{1t}}{(1 + \nabla Z_0 \cdot \nabla Z_0)^{1/2}}, \tag{A3}$$

where $2H_1$ is the perturbation of $2H$. On the reference domain we have

$$\rho \frac{\partial \vec{v}_1}{\partial t} = \nabla \cdot \vec{\vec{T}}_1, \quad \nabla \cdot \vec{v}_1 = 0 \tag{A4}$$

and

$$\iint_{\mathcal{A}} Z_1 \, dx \, dy = 0.$$

We assume a solution

$$\vec{v}_1(x,y,z,t) = e^{\sigma t}\vec{v}_1(x,y,z), \quad Z_1 = e^{\sigma t} Z_1(x,y), \quad \text{etc.},$$

hence on the domain we have

$$\rho\sigma \vec{v}_1 = \nabla \cdot \vec{\vec{T}}_1, \quad \nabla \cdot \vec{v}_1 = 0. \tag{A5}$$

Then dotting this with $\vec{v}_1^*$, the complex conjugate of $\vec{v}_1$, and integrating over the domain we obtain

$$\rho\sigma \int_{V_0} \vec{v}_1 \cdot \vec{v}_1^* \, dV_0 = -\int_{S_0} dA_0 \, \vec{n}_0 \cdot \vec{\vec{T}}_1 \cdot \vec{v}_1^* - 2\mu \int_{V_0} \vec{\vec{D}}_1 : \vec{\vec{D}}_1^* \, dV_0,$$

where $\vec{n}_0$ is inward and where S_0 denotes the surface of the reference drop.

Along S_0, $\vec{v}_1$ defines its own tangent and we write

$$\vec{v}_1 = \vec{n}_0(\vec{n}_0 \cdot \vec{v}_1) + \vec{t}_0(\vec{t}_0 \cdot \vec{v}_1),$$

whereupon we obtain

$$\rho\sigma \int_{V_0} \vec{v}_1 \cdot \vec{v}_1^* \, dV_0 = \int_{S_0} dA_0 \, (\gamma 2H_1 + \rho g Z_1) \frac{\sigma^* Z_1^*}{(1 + \nabla Z_0 \cdot \nabla Z_0)^{1/2}} - 2\mu \int_{V_0} \vec{\vec{D}}_1 : \vec{\vec{D}}_1^* \, dV_0.$$

Likewise we have

$$\rho\sigma^* \int_{V_0} \vec{v}_1^* \cdot \vec{v}_1 \, dV_0 = \int_{S_0} dA_0 \, (\gamma 2H_1^* + \rho g Z_1^*) \frac{\sigma \, Z_1}{(1 + \nabla Z_0 \cdot \nabla Z_0)^{1/2}} - 2\mu \int_{V_0} \vec{\vec{D}}_1^* : \vec{\vec{D}}_1 \, dV_0,$$

where

$$\int_{S_0} dA_0 \frac{1}{(1 + \nabla Z_0 \cdot \nabla Z_0)^{1/2}} [(\gamma 2H_1 + \rho g Z_1)\sigma^* Z_1^*] = \int_{\mathcal{A}} dx \, dy [(\gamma 2H_1 + \rho g Z_1)\sigma^* Z_1^*].$$

What we wish to know is: if $\mathrm{Re}\,\sigma = 0 = \mathrm{Re}\,\sigma^*$, is $|\vec{v}_1| = 0$? Now we have Eq. (4), *viz.*,

$$2H_1 = \mathcal{L} Z_1,$$

whereupon we can write

$$\rho \, \mathrm{Re}(\sigma) \int_{V_0} |\vec{v}_1|^2 dV_0 = \int_{\mathcal{A}} dx \, dy (\gamma \mathcal{L} Z_1 + \rho g Z_1) \, \mathrm{Re}(\sigma) Z_1^* - 2\mu \int_{V_0} dV_0 \, \vec{\vec{D}}_1 : \vec{\vec{D}}_1^*,$$

where $Z_1^* \mathcal{L} Z_1$ is positive. Hence $\mathrm{Re}(\sigma) = 0$ implies $\vec{v}_1 = \vec{0}$ whereupon $\sigma = 0$ due to Eq. (A3).

APPENDIX B: POTENTIAL ENERGY (NOT SCALED)

Our aim is to derive the equation for a neutral displacement of a drop by taking account of potential energy changes.

The potential energy of a drop of shape $z = Z(x,y)$, where (x,y) is a point on a domain $\mathcal{A}$ in the x,y plane bounded by a curve $\mathcal{C}$, is

$$\mathrm{PE}(Z) = \int_{\mathcal{A}} \left\{ \gamma (1 + \nabla Z \cdot \nabla Z)^{1/2} - \frac{1}{2} \rho g Z^2 \right\} dx\, dy, \tag{B1}$$

and its volume is

$$V = -\int_{\mathcal{A}} Z\, dx\, dy.$$

Now we denote by $Z_0(x,y)$ a solution to our drop-shape problem, *viz.,* Eqs. (1)–(3), corresponding to an input volume V_0. And we subject Z_0 to a displacement εZ_1, holding the volume of the drop constant, where $Z_1 = 0$ on $\mathcal{C}$ and

$$\int_{\mathcal{A}} Z_1\, dx\, dy = 0.$$

Hence we find

$$\begin{aligned} \mathrm{PE}(Z_0 + \varepsilon Z_1) - \mathrm{PE}(Z_0) = \varepsilon \int_{\mathcal{A}} \left\{ \gamma \frac{\nabla Z_0}{(1 + \nabla Z_0 \cdot \nabla Z_0)^{1/2}} \cdot \nabla Z_1 - \rho g Z_0 Z_1 \right\} dx\, dy \\ + \frac{1}{2} \varepsilon^2 \int_{\mathcal{A}} \left\{ \gamma \frac{\nabla Z_1 \cdot \nabla Z_1 (1 + \nabla Z_0 \cdot \nabla Z_0) - \nabla Z_0 \cdot \nabla Z_1 \nabla Z_0 \cdot \nabla Z_1}{(1 + \nabla Z_0 \cdot \nabla Z_0)^{3/2}} \right. \\ \left. - \rho g Z_1^2 \right\} dx\, dy + \cdots . \end{aligned} \tag{B2}$$

The first term on the right-hand side, due to $Z_1 = 0$ on $\mathcal{C}$, is

$$\varepsilon \int_{\mathcal{A}} \left\{ -\gamma \nabla \cdot \frac{\nabla Z_0}{(1 + \nabla Z_0 \cdot \nabla Z_0)^{1/2}} - \rho g Z_0 \right\} Z_1\, dx\, dy,$$

and this is zero in view of Eqs. (1) and (3).

The second term is

$$\frac{1}{2} \varepsilon^2 \int_{\mathcal{A}} \left\{ \gamma \frac{\nabla Z_1 \cdot \nabla Z_1 + \nabla Z_1 \cdot \nabla Z_1\, \nabla Z_0 \cdot \nabla Z_0 - (\nabla Z_1 \cdot \nabla Z_0)^2}{(1 + \nabla Z_0 \cdot \nabla Z_0)^{3/2}} - \rho g Z_1^2 \right\} dx\, dy,$$

and it is made up of a stabilizing positive part due to the increase in surface potential energy and a destabilizing negative part due to the decrease in gravitational potential energy. Thus, if $g = 0$, Z_0 is always stable. If $\gamma = 0$, Z_0 is always unstable.

Now if Z_1 is a neutral displacement of Z_0, the second term must be zero and to see what this requires of Z_1, we write the second term

$$\begin{aligned} \frac{1}{2} \varepsilon^2 \int_{\mathcal{A}} \left[\gamma \left\{ \frac{\nabla Z_1 (1 + \nabla Z_0 \cdot \nabla Z_0) - \nabla Z_0 \cdot \nabla Z_1 \nabla Z_0}{(1 + \nabla Z_0 \cdot \nabla Z_0)^{3/2}} \right\} \cdot \nabla Z_1 - \rho g Z_1^2 \right] dx\, dy \\ = \frac{1}{2} \varepsilon^2 \int_{\mathcal{A}} \left[-\gamma \nabla \cdot \left\{ \frac{\nabla Z_1 (1 + \nabla Z_0 \cdot \nabla Z_0) - \nabla Z_0 \cdot \nabla Z_1 \nabla Z_0}{(1 + \nabla Z_0 \cdot \nabla Z_0)^{3/2}} \right\} Z_1 - \rho g Z_1^2 \right] dx\, dy \end{aligned}$$

$$= \frac{1}{2}\varepsilon^2 \int_{\mathcal{A}} \left[-\gamma \nabla \cdot \left\{ \frac{\overrightarrow{I}(1+\nabla Z_0 \cdot \nabla Z_0) - \nabla Z_0 \nabla Z_0}{(1+\nabla Z_0 \cdot \nabla Z_0)^{3/2}} \cdot \nabla Z_1 \right\} - \rho g Z_1 \right] Z_1 \, dx \, dy$$

$$= \frac{1}{2}\varepsilon^2 \int_{\mathcal{A}} (-\gamma \mathcal{L} Z_1 - \rho g Z_1) Z_1 \, dx \, dy.$$

And for this to be zero, no matter Z_0, we see that Z_1 must satisfy Eq. (4).

The potential energy calculation applies to experiment I. It is the starting point for, e.g., Maddocks [15] and Lowry and Steen [16], and others.

Experiment II is little different. Due to the effect of gravity, it can not be obtained from experiment I by switching the roles of P and V.

APPENDIX C: UPWARD FORCE

We have a drop pinned along a curve $\mathcal{C}$ bounding a region $\mathcal{A}$ in the x,y plane. Its surface is denoted S. The outward normal to $\mathcal{C}$ in the x,y plane is $\frac{\nabla Z}{(\nabla Z \cdot \nabla Z)^{1/2}}$. We have a solution $Z(x,y,B,V)$ to our drop-shape problem and integrating Eq. (1) over $\mathcal{A}$ gives us

$$PA + BV = \int_{\mathcal{C}} ds \, \frac{\overrightarrow{n} \cdot \nabla Z}{(1+\nabla Z \cdot \nabla Z)^{1/2}} = \int_{\mathcal{C}} ds \, \frac{(\nabla Z \cdot \nabla Z)^{1/2}}{(1+\nabla Z \cdot \nabla Z)^{1/2}}.$$

Along $\mathcal{C}$ we have

$$\frac{\overrightarrow{k} - \nabla Z}{(1+\nabla Z \cdot \nabla Z)^{1/2}} : \text{ normal to } S \text{ at } \mathcal{C},$$

$$\frac{\nabla Z}{(\nabla Z \cdot \nabla Z)^{1/2}} : \text{ normal to } \mathcal{C} \text{ in the } x\text{-}y \text{ plane},$$

$$\frac{\nabla Z \times \overrightarrow{k}}{\nabla Z \cdot \nabla Z} : \text{ tangent to } \mathcal{C} \text{ in the } x\text{-}y \text{ plane},$$

and we need the tangent to S at $\mathcal{C}$ perpendicular to $\mathcal{C}$. It is

$$\frac{\nabla Z + \overrightarrow{k}(\nabla Z \cdot \nabla Z)}{(\nabla Z \cdot \nabla Z)^{1/2}(1+\nabla Z \cdot \nabla Z)^{1/2}}.$$

Hence the upward force of $\mathcal{C}$ on the surface of the drop is

$$\int_{\mathcal{C}} ds \, \frac{(\nabla Z \cdot \nabla Z)^{1/2}}{(1+\nabla Z \cdot \nabla Z)^{1/2}},$$

and we see that the upward force of the curve $\mathcal{C}$, along which the drop is pinned, on the drop vanishes if and only if ∇Z is pointwise zero.

APPENDIX D: MANY WAYS TO RUN A PRESSURE CONTROLLED DROP EXPERIMENT

Figure 13 is a sketch of a pressure-controlled drop experiment

The tube is assumed always to be full of more dense fluid and the volumes, V_1 and V_2, are the volumes above $z = 0$.

The drop experiment is hydrostatic and P is the input, $Z(x,y)$ is the output.

The pressures P_1 and P_2, are

$$P_1 = P + P_{\text{atm}} + \rho_1 g h_1 - \rho_1 g Z \tag{D1}$$

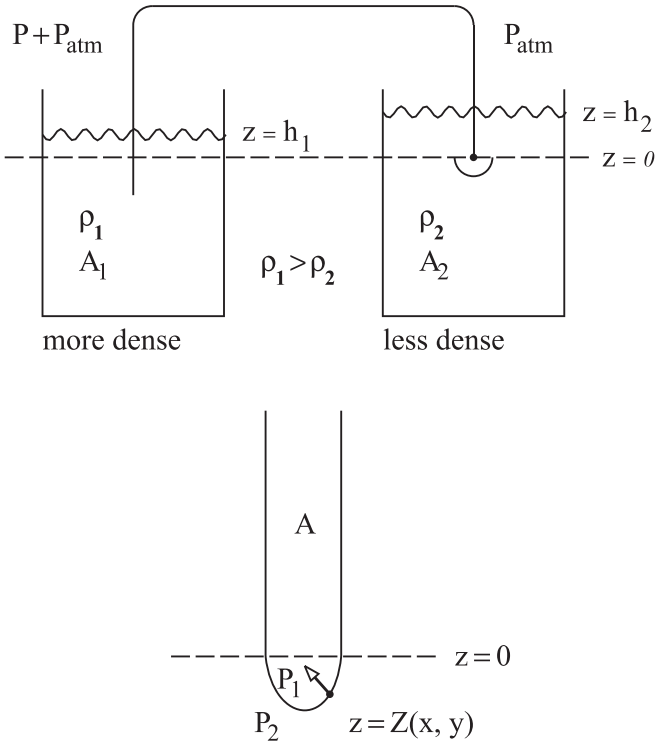

FIG. 13. Sketch of a pressure-controlled drop experiment.

and

$$P_2 = P_{\text{atm}} + \rho_2 g h_2 - \rho_2 g Z \tag{D2}$$

whereupon Z, the drop shape, i.e., base shape is obtained by solving

$$\gamma\, 2H(Z) = P_1 - P_2 = P + \rho_1 g h_1 - \rho_2 g h_2 - (\rho_1 - \rho_2) g Z. \tag{D3}$$

Now h_1 and h_2 depend on the pressure and can be eliminated by observing:
(1) At $Z = 0$ we have $P = P_0$, $h_1 = h_{10}$, and $h_2 = h_{20}$ where $P_0 + \rho_1 g h_{10} - \rho_2 g h_{20} = 0$
(2) Thus we have

$$\gamma\, 2H = P - P_0 + \rho_1 g (h_1 - h_{10}) - \rho_2 g (h_2 - h_{20}) - (\rho_1 - \rho_2) g Z \tag{D4}$$

and
(3)

$$A_1 h_1 - \iint Z\, dx\, dy = A_1 h_{10} \tag{D5}$$

and

$$A_2 h_2 + \iint Z\, dx\, dy = A_2 h_{20}, \tag{D6}$$

whereupon Z satisfies

$$\gamma\, 2H(Z) = P + \rho_1\, g\, \frac{1}{A_1} \iint Z\, dx\, dy + \rho_2\, g\, \frac{1}{A_2} \iint Z\, dx\, dy - (\rho_1 - \rho_2) g Z, \tag{D7}$$

and P is now $P - P_0$.

If A_1 and A_2 are very large we have

$$\gamma\, 2H(Z) = P - (\rho_1 - \rho_2) g Z, \tag{D8}$$

and the corresponding eigenvalue problem is our diffusion eigenvalue problem. This is Wente's statement of the static drop problem wherein critical points are always turning points [13].

Now if $A_1 = A$, i.e., the left-hand tank is simply a pipe, we have

$$\gamma\, 2H(Z) = P + \rho_1\, g\, \frac{1}{A} \iint_A Z\, dx\, dy + \rho_2\, g\, \frac{1}{A_2} \iint_A Z\, dx\, dy - (\rho_1 - \rho_2) g Z \tag{D9}$$

And thus if A_2 is very large we have

$$\gamma\, 2H(Z) = P + \rho_1\, g\, \frac{1}{A} \iint_A Z\, dx\, dy - (\rho_1 - \rho_2) g Z. \tag{D10}$$

This is our statement of experiment II in unscaled variables.

Hence the diffusion eigenvalue problem has a definite physical connection to all drop experiments, but even if it had not, nothing would have been lost. The diffusion eigenvalues are based on drop shapes found in experiments I and II, not on shapes found in Wente's thought experiment.

APPENDIX E: DERIVATION OF THE BASE EQUATIONS

1. Experiment I

We have

$$\vec{g} = -g\, \vec{k} \tag{E1}$$

and

$$\frac{dP}{dz} = -\rho\, g, \tag{E2}$$

whereupon

$$P = -\rho g z + C, \tag{E3}$$

$$P* = -\rho * g z + C*, \tag{E4}$$

$$P(h) = -\rho g h + C, \tag{E5}$$

and

$$P(-h*) = \rho g h * + C*. \tag{E6}$$

At $z = Z$ we have

$$P* + \gamma\, 2H = P, \tag{E7}$$

whereupon

$$\gamma\, 2H = -(\rho - \rho*) g Z + C - C*, \tag{E8}$$

where

$$C - C* = P(h) + \rho g h - [P(-h*) - \rho g h*], \tag{E9}$$

and scaling produces Eq. (1).

2. Experiment II

Unlike experiment I, it is not the volume of the drop that remains constant on perturbation. This is important in the presence of gravity. Again we have at $z = Z$

$$P + \rho g h - \rho g Z - (P_{\text{atm}} + \rho * g h * - \rho * g Z) = \gamma\, 2H. \tag{E10}$$

Denoting h and P by h_0 and P_0 when $Z = 0$, we have

$$P_0 - \rho g h_0 - (P_{\text{atm}} + \rho g h *) = 0, \tag{E11}$$

whereupon, eliminating $P_{\text{atm}} + \rho g h *$, using

$$(h_0 - h)A = -\iint_a Z\, dx\, dy, \tag{E12}$$

and scaling we have Eq. (11).

[1] D. H. Michael, Meniscus stability, Annu. Rev. Fluid Mech. **13**, 189 (1981).

[2] A. D. Myshkis, V. G. Babskii, N. D. Kopachevskii, L. A. Slobozhanin, and A. D. Tyuptsov, *Low-Gravity Fluid Mechanics* (Springer, New York, 1987).

[3] L. A. Slobozhanin and A. D. Tyuptsov, Characteristic stability parameter of the axisymmetric equilibrium surface of a capillary liquid, Fluid Dynamics **9**, 563 (1974).

[4] L. A. Slobozhanin and J. I. D. Alexander, The stability of two connected drops suspended from the edges of circular holes, J. Fluid Mech. **563**, 319 (2006).

[5] J. C. Maxwell, *The Scientific Papers*, Vol. 2 (Cambridge University Press, Cambridge, 1927), pp. 541–591.

[6] S. R. Majumdar and D. H. Michael, The equilibrium and stability of two-dimensional pendent drops, Proc. R. Soc. London A **351**, 89 (1976).

[7] E. Pitts, The stability of pendant liquid drops. Part 1. Drops formed in a narrow gap, J. Fluid Mech. **59**, 753 (1973).

[8] E. Pitts, The stability of pendant liquid drops. Part 2. Axial symmetry, J. Fluid Mech. **63**, 487 (1974).

[9] D. H. Michael and P. G. Williams, The equilibrium and stability of axisymmetric pendent drops, Proc. R. Soc. London A **351**, 117 (1976)

[10] L. E. Johns and R. Narayanan, *Interfacial Instability* (Springer, New York, 2002).

[11] G. C. Mason, An experimental determination of the stable length of cylindrical liquid bubbles, J. Colloid Interface Sci. **32**, 172 (1970).

[12] X. Lin, Stability of the pendent drop and the enclosed liquid bridge, Ph.D. thesis, University of Florida, 2016.

[13] H. C. Wente, The stability of the axially symmetric pendent drop, Pac. J. Math. **88**, 421 (1980).

[14] J. Eggers, Nonlinear dynamics and breakup of free-surface flows, Rev. Mod. Phys. **69**, 865 (1997).

[15] J. H. Maddocks, Stability and folds, Proc. R. Soc. London A **449**, 411 (1995).

[16] B. Lowry and P. H. Steen, Capillary surfaces: Stability from families of equilibria with application to the liquid bridge, Arch. Rational Mech. Anal. **99**, 301 (1987).